



25th International Conference on Fracture and Structural Integrity

Room temperature creep mechanism of a Pb-Sn-Sb lead alloy

Luigi Mario Viespoli^{a*}, Audun Johanson^b, Antonio Alvaro^c, Bård Nyhus^c, Filippo Berto^a

^aDepartment of Mechanical and Industrial Engineering, Norwegian University of Science and Technology (NTNU), Norway

^bNexans Norway, Innspurten 9, 0663 Oslo, Norway

^cSintef Industry, Richard Birkelands vei 2B, 7031, Trondheim, Norway

Abstract

Lead alloys are the most common materials adopted for the production of subsea power cable sheathing. The sheathing is a layer of stable and watertight metal, which serves to prevent the electrical failure of the cable. During the predicted operational life of the cables of several decades, these experience strains due to the installation process, the oceanic currents and the thermal expansion of the cable. The low melting temperature of such alloys, around 600 K, imply that creep deformation will occur when subjected to loading even at room temperature. The goal of the present study is to investigate the tensile behavior of the Pb-Sb-Sn alloy of interest in order to predict the correlation between strain rate and stress level. A mechanical characterization was performed through tensile testing at different strain rates of specimens cut from power cable sheathing. Due to the extreme ductility of the material, the use of digital image correlation was necessary to compute an acceptable approximation of the in-plane strain field on the surface of the specimens. The results were implemented in finite element method environment using Abaqus and Isight to calibrate a creep model able to reproduce at best the behavior of the material. Such model was also positively tested in the case of a relaxation test. In addition, a tensile test of several steps at different loads was executed with the aim of extrapolating and interpreting the steady state creep exponents at different creep regimes and the indications that these can provide on the deformation mechanisms of the alloy.

© 2019 The Authors. Published by Elsevier B.V.

Peer-review under responsibility of the Gruppo Italiano Frattura (IGF) ExCo.

Keywords: lead; creep; plasticity mechanisms; modelling; digital image correlation

* Corresponding author. Tel.: +47-459-13-281

E-mail address: luigi.m.viespoli@ntnu.no

1. Introduction

Power cables used for submarine applications necessitate a watertight layer to prevent failure from electrical short circuit. Due to their properties of chemical stability and ductility, lead alloys have been employed for decades for the manufacturing of the sheathing layer. Due to the melting point inferior to 600 K, such alloys operate in a relatively high temperature regime. Creep deformation, stress relaxation and recrystallization are phenomena relevant at room temperature operation, Kassner et al (2015). Similar materials have been often studied in the microelectronics field, in which the interest is focused on the creep-fatigue interaction of solders, Pang et al. (1998), Lall et al. (2015), Motalab et al. (2012). Creep mechanisms which depend on grain boundary sliding present an increased resistance to deformation and a higher yield stress for an increased grain size, Fargalli et al. (1974), Kassner et al. (2000), Viespoli et al. (2019). Most of the research on the specific topic of the creep and fatigue behavior of lead alloys for the production of cable sheathing reaches to several decades ago, Feltham et al. (1956), Sahota et al. (2000), Harvard (1972), Dollins and Betzer (1956), Anelli et al. (1986). Up to date design has been performed on the base of experience and acquired know how. New interest for this research has in the recent years risen from the industry with the aim of a deeper understanding of the mechanisms driving the deformation and damage, Johanson et al. (2018), of such alloys for a more conscious, efficient and sustainable production. The manuscript presents the result of a series of tensile tests giving insight on the deformation mechanisms possibly active during the installation and operation of the power-line, which sees decades of low strain rate, strain controlled deformation cycles caused by sea currents and tides and thermal cycling due to the periodic power request.

2. Material tensile characterization and modelling

2.1. Anand creep model

For the numerical reproduction of the mechanical response of a metallic alloy subjected to creep deformation at elevated temperature several models have been proposed. Of these, the one proposed by Anand, Anand (1982), Brown et al. (1989), is able to reproduce the creep behavior in the primary and secondary stage, that is the steady state creep regime. The constitutive equations characterizing the model include the effects of both temperature and strain hardening. The stress-strain correlation is expressed by the flow equation:

$$\dot{\bar{\epsilon}}^{cr} = A \cdot \exp(-Q/R(\theta - \theta^z)) \left[\sinh(\xi \bar{q}/s) \right]^{1/m} \quad (1)$$

The different parameters included in the equation above are:

A , pre-exponential factor;

Q , activation energy;

m , strain rate sensitivity exponent;

R , universal gas constant;

ξ , material parameter;

θ^z , absolute temperature value;

\bar{q} , uniaxial equivalent deviatoric stress

$\dot{\bar{\epsilon}}^{cr} = \sqrt{2/3} \dot{\epsilon}^{cr} : \dot{\epsilon}^{cr}$, uniaxial equivalent creep strain rate.

The response of the material depends on an internal value s , which is dimensionally a stress and corresponds to the resistance opposed to the plastic flow. The evolution of this variable considers strain hardening and recovery in the form:

$$\dot{s} = h_0 |1 - s/s^*|^a \operatorname{sign}(1 - s/s^*) \dot{\varepsilon}^{cr} \quad (2)$$

Being:

$$s^* = \hat{s} \left[\dot{\varepsilon}^{cr} / A \cdot \exp(Q/R(\theta - \theta^z)) \right]^n \quad (3)$$

And:

$$h_0 = A_0 + A_1(\theta - \theta^z) + A_2(\theta - \theta^z)^2 + A_3 \dot{\varepsilon}^{cr} + A_4 (\dot{\varepsilon}^{cr})^2 \quad (4)$$

While the initial deformation resistance is:

$$s_0 = S_1 + S_2(\theta - \theta^z) + S_3(\theta - \theta^z)^2 \quad (5)$$

s^* is the saturation value of s at a certain strain rate and temperature. h_0 is the strain rate or softening constant, \hat{s} is a coefficient and a and n are material dependent. The Anand creep model implemented in the finite element modelling software Abaqus is modified with the addition of the six parameters $A_1, A_2, A_3, A_4, S_2, S_3$, SIMULIA User Assistance (2017).

2.2. Tensile testing and creep model calibration

Before the determination of the steady state creep exponents of the material, a tensile investigation and numerical calibration of the Anand model were executed, Viespoli et al. (2019). The lead alloy object of the investigation in the present work is an E alloy the composition of which is reported in Table 1. The material was received in the form of extruded tubes of 82 mm of diameter and 3.3 mm of wall thickness. Such tubes constitute the sheathing layer, that is the watertight barrier and provides electrical short-circuit failure resistance to the subsea power cable. The alloy was cut and unfolded from a power cable section and machined to obtain the dog-bone geometry in Figure 1 a. For computing the real longitudinal strain of the material, overcoming the practical challenges caused by the elevated ductility of the alloy, the digital image correlation (DIC) technique was used, recording the tests with a Prosilica GC 2450 digital camera and post processing the results with the software eCorr, Figure 1 b and 1 c. To obtain the response of the alloy tensile testing at nominal strain rates of 1E-3, 1E-5 and 1E-7 s-1 and a relaxation test from the stress of 10 MPa were performed. The nominal strain rates were computed as the displacement speed of the testing machine clamps divided by the constant width length of the specimens, that is 44 mm. The results of the four tests were connected though an I sight loop with equivalent models realized in Abaqus environment, Figure 2 b, to calibrate the parameters of the Anand model. The Figures 2 a and c demonstrate the good agreement between the experimental results and the numerical model.

Table 1. Alloy chemical composition, weight percentage.

Pb	Sb	Sn
99.3	0.2	0.5

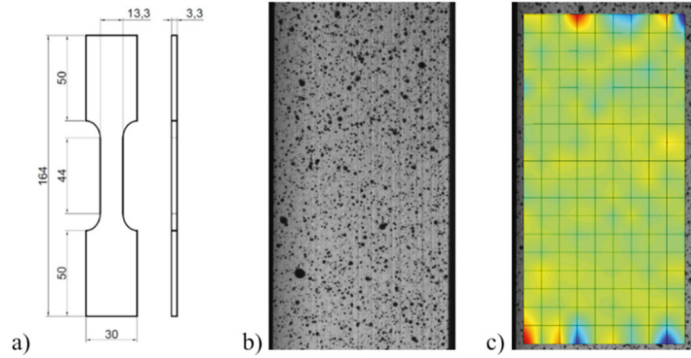


Fig. 1. (a) Specimen geometry (a); speckle pattern (b); DIC mesh and longitudinal strain pattern, which is homogeneous in the central section of the specimen (c).

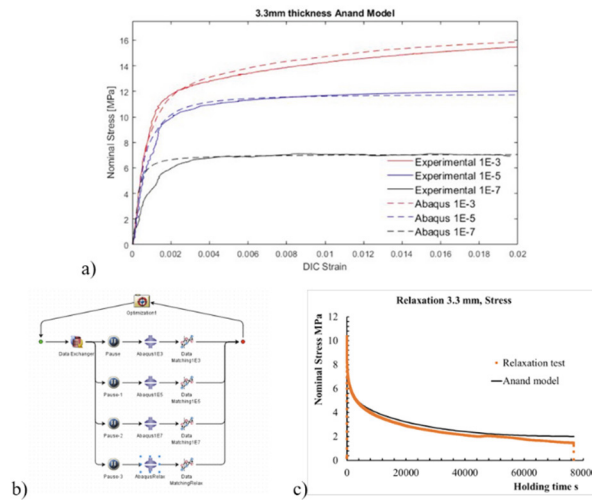


Fig. 2. (a) Tensile test and Anand creep model results; (b) Isight optimization loop; (c) relaxation test and Anand creep model results [7].

3. Creep mechanism investigation

3.1. Tensile testing and creep model calibration

Creep deformation can be caused by several different mechanism according to the material and the stress level active on the metal lattice. According to Dowling (1993) an exponential correlation exists between the stress applied and the resulting steady state creep rate in the form of:

$$\dot{\epsilon} = A_2 \sigma^m / d^q T \cdot \exp(-Q/RT) \tag{6}$$

The variables influencing the strain rate are the stress σ , the temperature T and the average grain diameter d . The remaining parameters, that is the coefficient A_2 , the exponents m and q and the activation energy Q depend on the material and on the creep mechanism active. In the case of low stress, but relatively elevated temperature, diffusional flow is active. This is characterized by $m=1$ and $q=2$ for vacancy diffusion through the crystal lattice and $q=3$ for

vacancy diffusion along grain boundaries. The mechanism of grain boundary sliding is indicated by a value of the exponent equal to $m=2$, with the exponent q assuming the same values and meaning as in the former case. At more elevated stress levels the mechanism of dislocation creep is active. Dislocation motion creep is indicated by an exponent m assuming values between 3 and 8, while $q=0$, that is a negligible dependence on the average grain size. For the tested alloy, the last point appears to be in contrast with the experimental evidence reported by Viespoli et al. (2019), in which the grain size influences the response also in the dislocation creep regime.

Table 2. Alloy chemical composition, weight percentage.

Step	Initial Stress [MPa]	Target Stress [MPa]	Time [s]	Initial Strain	Final Strain
1	0	8,5	250	0	0,001404836
2	8,5	8,5	15000	0,001404836	0,009813991
3	8,5	6	250	0,009813991	0,009658554
4	6	6	30000	0,009658554	0,010542822
5	6	5	250	0,010542822	0,010495558
6	5	5	30000	0,010495558	0,010825471
7	5	4	250	0,010825471	0,010778678
8	4	4	30000	0,010778678	0,010930828
*9	4	1,48	25000	0,010930828	0,010726642
10	1,48	-3	250	0,010726642	0,010356466
11	-3	-3	30000	0,010356466	0,009811369
12	-3	3	250	0,009811369	0,010246884
13	3	3	30000	0,010246884	0,010655562
14	3	-5	250	0,010655562	0,010003737
15	-5	-5	30000	0,010003737	0,008979056
16	-5	5	250	0,008979056	0,009693417
17	5	5	205200	0,009693417	0,013166749

3.2. Step test results

In order to understand the fundamental mechanisms at the base of the creep deformation of the lead alloy it is then important to obtain the steady state creep exponent relating the applied stress to the strain rate. For collecting the necessary data to have information on the material behavior, a tensile test composed of several steps was executed. The specimen geometry and base material for this test were the same used in the initial tensile characterization for model calibration and the DIC technique was used to obtain the total longitudinal strain of the material. The different steps in the test, described in Table 2, were planned in terms of stress and time to provide results on the steady state creep behavior at different creep regimes. The deformation obtained in during the test is plotted against the time in Figure 3. The slope of each of the steps in positive (tensile) stress was determined in the regions in which the correlation between the strain and the time elapsed is linear, that is in steady state creep regime. The values of the steady state strain rate and the corresponding constant stress applied are plotted in Figure 4. To these values, two points are added from the tensile testing at a nominal strain rate of $1E-5$ and $1E-7$ s⁻¹ reported in Figure 2 a. In these two tests at constant strain rate the applied stress reaches a constant value, conditions which corresponds do second stage creep. From the results obtained three regimes can be distinguished, characterized by three different stress exponents m . In the range 6 to 12 MPa the value found is $m=8.43$. This value is at the high end of the dislocation climb dominated creep deformation. In the range 5 to 6 MPa the exponent assumes the value $m=5.52$, lower but still in the range of the same deformation mechanism. For the lowest range of stress object of the test, that is between 3 and 5 MPa, and exponent $m=0.907$ is computed. This value is compatible with the diffusional creep mechanisms of vacancy diffusion along the grain boundaries of through the crystal lattice. To assess which of the two mechanisms is

predominant it would be necessary to produce new results for the material in condition of different grain size, assessing then the value of the exponent q .

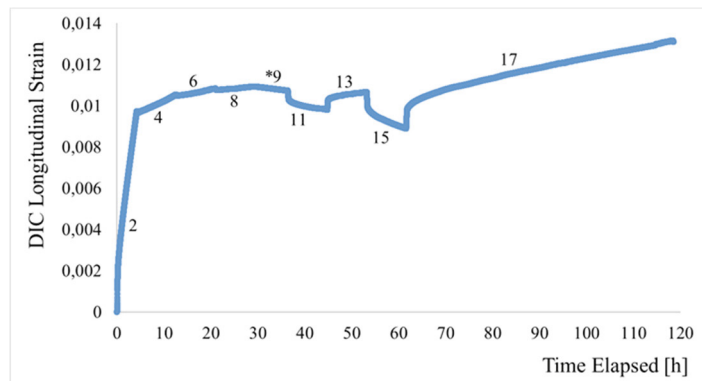


Fig. 3. Longitudinal DIC strain obtained in the step test. The numbers indicate the steps, *9 being the relaxation step.

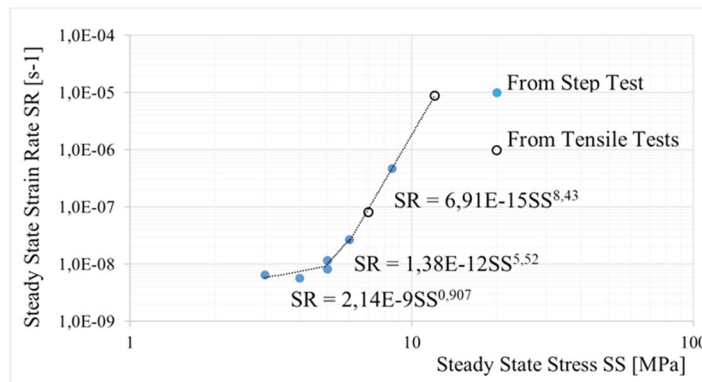


Figure 4. Steady state creep regimes and relative exponents as obtained from the analysis of the step test points in positive stress, plus the results of the tensile testing in which constant stress is reached.

4. Conclusions

The present work is the synthesis of a series of tests on dog-bone specimens of a lead E alloy industrially used for the production of the sheathing layer of subsea power cables. Firstly, the three tests at different nominal strain rates plus a relaxation test were performed to characterize the strain rate sensitivity caused by the creep mechanisms active and to calibrate the parameters of a numerical model based on the Anand creep model, which successfully approximated the mechanical response of the alloy to the deformation imposed. To study the mechanisms active during the time dependent deformation of the alloy the steady state creep behavior was investigated. From the results of a tensile test composed of several steps at different stress levels, each of which reached the secondary creep stage, the exponent correlating stress and strain rate for steady state creep was obtained between 3 and 12 MPa. The values assumed by such material parameter in the range of interest indicate that mechanisms of diffusional creep are active in the low stress range of 3 to 5 MPa, with a value of the exponent close to 1, while dislocation creep is the dominating mechanism for higher stresses, with values ranging from 5.5 to 8.4. Further testing for different average grain size would then be necessary in the low stress range to determine whether vacancy diffusion through the crystal lattice or vacancy diffusion along the grain boundaries is predominant.

Acknowledgements

The present work was financed by Nexans Norway AS and the Research Council of Norway (IPN in ENERGIX Project number 256367) and performed within the project: Next-generation damage based fatigue of cable sheathing (REFACE).

References

- Kassner, M.E. *Fundamentals of Creep in Materials* (Third Edition). Butterworth-Heinemann, 2015.
- Pang, H.L.J., Wang, Y.P., Shi X.Q., Wang, Z.P. Sensitivity study of temperature and strain rate dependent properties on solder joint fatigue life. *Proceedings of 2nd Electronics Packaging Technology Conference*, pp. 184-189, 1998.
- Lall, P., Zhang, D., Yadav, V., Locker, D. High Strain-Rate Constitutive Behavior of SAC105 and SAC305 Lead-free Solder, *IEEE*, 2015.
- Motalab, M., Cai, Z., Suhling, J.C., Lall, P., Determination of Anand constants for SAC solders using stress-strain or creep data. *13th InterSociety Conference on Thermal and Thermomechanical Phenomena in Electronic Systems*, San Diego, CA, pp. 910, 2012.
- Mohamed, F.A., Langdon, T.G. The transition from dislocation climb to viscous glide in creep of solid solution alloys, *Acta Metallurgica*, Volume 22, Issue 6, pp. 779-788, 1974.
- Kassner, M.E. *Five-power-law creep in single phase metals and alloys*. Oxford: Pergamon, 2000.
- Viespoli, L.M., Johanson, A., Alvaro, A., Nyhus, B., Sommacal, A., Berto, F. Tensile characterization of a lead alloy: creep induced strain rate sensitivity. *Materials Science and Engineering: A*, Volume 744, pp. 365-375, 2019.
- Feltham, P. On the Mechanism of High-Temperature Creep in Metals with Special Reference to Polycrystalline Lead. *Proc Phys Soc*, 69,12-B, 1956.
- Sahota, M.K., Riddington, J.R. Compressive creep properties of lead alloys. *Materials and Design*, 21: 159-167, 2000.
- Harvard, D.G. *Fatigue of Lead Cable-Sheathing Alloys*. Ontario Hydro research, 1972.
- Dollins, C.W., Betzer, C.E. Creep Fracture and Bending of Lead and Lead Alloy Cable Sheathing. *Engineering experiment station bulletin* 440, 1956.
- Anelli, P., Donazzi, F., Lawson, W.G. The fatigue life of lead alloy E as a sheathing material for submarine power cables. *Societa' cavi Pirelli*, SM 393-3, 1986.
- Johanson, A., Viespoli, L.M., Nyhus, B., Alvaro, A., Berto, F. Experimental and numerical investigation of strain distribution of notched lead fatigue test specimen. *MATEC Web Conf*, 165, 2018.
- Anand, L., Constitutive Equations for the Rate-Dependent Deformation of Metals at Elevated Temperatures. *Journal of Engineering Materials and Technology*, Vol. 104(1), pp. 12-17, 1982.
- Brown, S., Kim, K., and Anand, L. An Internal Variable Constitutive Model for Hot Working of Metals. *International Journal of Plasticity*, Vol. 5(2), pp. 95-130, 1989.
- Dassault Systèmes, *SIMULIA User Assistance*, 2017.
- Dowling, N.E. *Mechanical Behavior of Materials: Engineering Methods for Deformation, Fracture, and Fatigue*. Pearson, 2013.